OPEN ACCESS
IOP Publishing
Superconductor Science and Technology
Supercond. Sci. Technol. **35** (2022) 055002 (16pp)
https://doi.org/10.1088/1361-6668/ac5c87

Enhanced critical axial tensile strain limit of CORC® wires: FEM and analytical modeling

V A Anvar[1,2,*], K Wang[1,3], J D Weiss[4], K Radcliff[5], D C van der Laan[4], M S A Hossain[2,6] and A Nijhuis[1,*]

[1] University of Twente, Faculty of Science and Technology, Enschede, The Netherlands
[2] Institute for Superconducting and Electronic Materials, University of Wollongong, Wollongong, Australia
[3] Department of Mechanics and Engineering Science, Lanzhou University, Lanzhou, Gansu 730000, People's Republic of China
[4] Advanced Conductor Technologies and University of Colorado, Boulder, CO, United States of America
[5] Advanced Conductor Technologies, Boulder, CO, United States of America
[6] University of Queensland, School of Mechanical and Mining Engineering, St Lucia, QLD, Australia

E-mail: v.a.anvar@utwente.nl and a.nijhuis@utwente.nl

Received 22 December 2021, revised 29 January 2022
Accepted for publication 10 March 2022
Published 22 March 2022

Abstract

Conductor on Round Core (CORC®) cables and wires are composed of spiraled high-temperature superconducting (HTS) rare-earth barium copper oxide (REBCO) tapes, wound in multiple layers, and can carry very high currents in background magnetic fields of more than 20 T. They combine isotropic flexibility and high resilience to electromagnetic and thermal loads. The brittle nature of HTS tapes limits the maximum allowable axial tensile strain in superconducting cables. An intrinsic tensile strain above about 0.45% will introduce cracks in the REBCO layer of straight HTS tapes resulting in irreversible damage. The helical fashion at which the REBCO tapes are wound around the central core allows tapes to experience only a fraction of the total axial tensile strain applied to the CORC® wire. As a result, the critical strain limit of CORC® wires can be increased by a factor of more than 10 that of REBCO tapes. Finite element (FE) and analytical models are developed to predict the performance of CORC® wires under axial tensile strain. A parametric analysis is carried out by varying the winding angle, the Poisson's ratio of the CORC® wire core, the core diameter, and the tape width. The results show that a small variation in winding angle can have a significant impact on the cable's axial tensile strain tolerance. While the radial contraction of the helically wound tapes in a CORC® wire under axial tensile strain depends on its winding angle, it is mostly driven by the Poisson's ratio of the central core, affecting the tape strain state and thus its performance. Contact pressure from multiple layers within the CORC® wire also affects the CORC® wire performance. The FE model can be used to optimize the cable design for specific application conditions, resulting in an irreversible strain limit of CORC® cables and wires as high as 7%.

* Authors to whom any correspondence should be addressed.

Keywords: CORC®, axial tensile strain, FEM, superconducting magnets, HTS cables, REBCO, critical strain

(Some figures may appear in color only in the online journal)

1. Introduction

High-temperature superconducting (HTS) technology enables compact fusion devices that potentially allow net fusion energy production in a relatively short time frame [1–3], and particle accelerator magnets that generate a dipole field exceeding 20 T. These applications often require a stable, highly flexible cable, that can withstand very high electromagnetic loads. Second-generation HTS tape or coated conductors are assembled into cables such as twisted stacked-tape cable [4], Roebel cables [5], and Conductor on Round Core (CORC®) cables and wires [6] for high current applications. Superconducting CORC® cables are manufactured by winding multiple layers of HTS rare-earth barium copper oxide (REBCO) tapes at alternate winding angles between layers. The winding process allows multiple layers of tapes to be assembled continuously, which is essential in producing long cables for many industrial applications. Unlike other common HTS cabling concepts, CORC® conductors can be bent in any direction, providing a higher degree of freedom in designing superconducting magnets. The central cylindrical core provides additional strength against tensile and transverse loads, which is essential to withstand high electromagnetic loads during operation. Axial tensile and transverse compressive loads up to the conductors critical stress were not detrimental to the CORC® cable performance even after 100 000 stress-cycles [7, 8].

Further improvement of the mechanical load limits of HTS cables is achieved by preventing the REBCO layer from undergoing irreversible degradation. Cracks will be formed on the thin (1–2 μm) brittle layer of REBCO if its intrinsic tensile strain exceeds 0.45% [9]. However, for R&D REBCO tapes, no irreversible limit on axial compressive strain was found until −2% strain was applied to the REBCO tape by soldering the tape onto a beam, followed by bending the beam in a four-point bender [10]. An irreversible strain limit under axial compression of about −1.2% is often measured when REBCO production tapes are wound into CORC® cables or wires [11, 12].

The effect of bending on the CORC® cable performance has been studied extensively using finite element (FE) modeling [13]. An FE model to study the tensile stress–strain characteristics and contact stress was developed by Wang *et al* [14]; it was found that the additional layers can increase the total contact stress experienced by the first layer and thus reduce the critical strain tolerance of the cable. Different types of loads acting on HTS tapes studied previously by Ilin *et al* [15] revealed that non-uniform copper layer deposition in HTS tapes can cause early degradation under transverse loads.

The advantage of CORC® cables and wires is that due to the helical shape of the tapes, HTS tapes in the conductors experience only a fraction of the total strain applied to the cable or wire. It was shown recently that the irreversible strain limit under axial tension of CORC® wires in which the tape winding angles were optimized exceeded 7%, which is more than ten times that of a straight REBCO tape [16]. The helical tape wind also means that the tensile strength of the tape is not fully transferred to the cable. Hence, CORC® cables with higher tensile strain tolerance come at the cost of a lower critical axial stress limit. However, the strength of the cable can be increased by using core materials with high yield strength, such as beryllium-copper, hardened copper or even stainless steel instead of annealed copper.

FE and analytical models are developed in this paper to calculate the strain state in the REBCO layers of the tapes wound into CORC® wires as a function of axial tensile strain applied to the CORC® wire. These models allow calculation of the applied strain at which the intrinsic strain limit of the REBCO tapes have been reached, resulting in irreversible performance degradation, for a wide range of parameters such as the tape winding angle, the tape width and the number of tape layers. The models are applied to explain the dependence of the critical current (I_c) on applied axial tensile strain of the CORC® wires reported in [16].

2. Modeling the strain state of REBCO tapes in CORC® conductors

2.1. FE model for axial tensile strain applied to CORC® wires

A detailed FE model is created in ABAQUS software. Before applying any mechanical load, the initial REBCO strain state is calculated after the tape production process and tape winding around the core to form the CORC® wire. A detailed description of all the steps involved and validation of the FE model for bending loads is explained in [13]. The manufacturer of the REBCO tape considered in this study is SuperPower Inc. The tape's production process involves the metal-organic chemical vapor deposition process, in which a thin REBCO layer is deposited on a Hastelloy substrate at 1020 K, then cooled to 350 K to deposit copper layers on both sides of the tape. After this, the tape is cooled to room temperature. The tape is modeled with multilayered shell elements due to the thin layer nature. The tape layers experience thermal strain due to the different coefficients of thermal expansion between matrix materials. The final shape of the tape after production is a spherical dome. The tape is then wound over a cylindrical core, usually copper. Then the whole CORC® cable or wire is cooled down to liquid nitrogen temperature. The modeling steps are shown in figure 1.

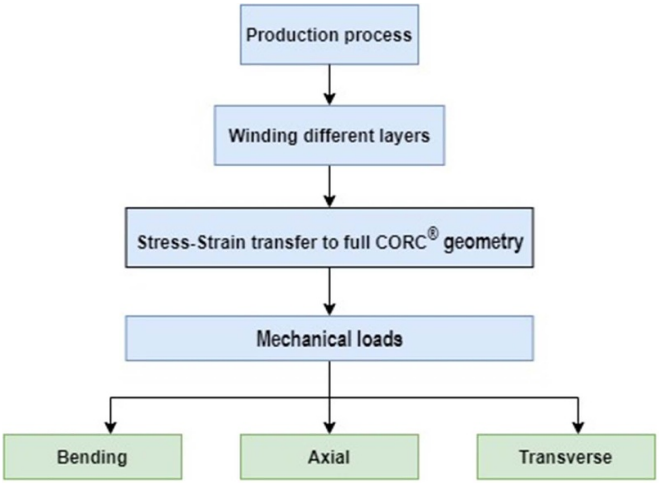

Figure 1. CORC® FE modeling steps for different types of mechanical loads.

Figure 2 shows the boundary conditions for axial load applied to the CORC® cable. The cable's total length is 60 mm, and the grip length is 5 mm on both ends of the cable. The tensile load is applied to the grips on both ends of the cable.

A four-node quadrilateral stress-displacement shell element (S4R) with reduced integration is used for the HTS REBCO tapes due to their thin nature, and an eight-node cubic-like element with reduced integration (C3D8R9) is used for the mesh of the core. The number of mesh elements along the length and width of the tape is selected after mesh optimization trials. Since for this study only the strain is important and not so much the stress behavior, the core is considered to be completely elastic. This consideration is valid for the tensile strain simulations since the diameter of the core after CORC® tensile load experiments [7] was found to be uniform throughout the cable's length. However, the elastoplastic properties of all layers of the HTS tape are taken into consideration. The material properties used for the FE analysis are listed in table 1.

The critical current of the HTS tape is calculated from the strain values of all the mesh elements. First, the strain data from the 240 × 12 element grid is converted to 1000 × 120 grid data using 2D spline interpolation. Next, the normalized critical current of tape, I_c/I_{c0} for each width section is calculated using equation (1) along the entire length of the tape [20]. It is assumed that the weakest section of the tape determines the critical current of the tape:

$$\frac{I_c}{I_{c0}} = \begin{cases} 1 - 6918|\varepsilon_i|^{2.2}, & \varepsilon_i < 0.45\% \\ 0, & \varepsilon_i \geqslant 0.45\% \end{cases}. \quad (1)$$

Here, ε_i is the intrinsic strain in the REBCO layer after the tensile load is applied to the cable. Any increase of critical current due to strain relaxation is not considered for estimating the critical strain limit of CORC® cables and wires.

2.2. Analytical model for axial tensile strain applied to CORC® wires

For ease of analysis, CORC® wires with REBCO tape wound around a copper core can be considered as a rectangular sheet with the tape on top, as shown in figure 3. As a result, only helical axial tension and radial contraction of the tapes in the CORC® wire under axial tension are considered; the effects of torsion, friction, contact force, and bending are not considered for the analytical model. The torsional strain is prominent only at small winding angles, defined at the angle between the tape and the direction normal to the CORC® wire core. The height of the rectangular sheet, πD is circumference of the core; here the thickness of the tape is neglected. The core diameter decreases when an axial load is applied to the CORC® wire, while the tape winding angle increases. The average strain state of the tape becomes tensile only if the tape closely follows the contraction of the core as the cable elongates. At very low winding angles, the tape either detaches from the core in the central part of the cable or experiences a compressive strain depending upon the peripheral constraints.

The axial strain state of the tape can be calculated as the ratio of the change in the tape's length after CORC® axial loading to the original tape's length and is formulated as equation (2):

$$\varepsilon_{tape} = (1+\varepsilon_a)^{-\mu} \times \frac{\cos(\alpha)}{\cos(\alpha_f)} - 1 \quad (2)$$

where, ε_a is the CORC® applied axial tensile strain, μ is the Poisson's ratio of the core, α is the initial winding angle and α_f is the final winding angle. The first part of the equation, $(1+\varepsilon_a)^{-\mu}$, represents the radial contraction, and the second part, $\frac{\cos(\alpha)}{\cos(\alpha_f)}$ represents the helical axial tension. The final winding angle α_f can be formulated as equation (3):

$$\alpha_f = \tan^{-1}\left(\frac{\tan(\alpha)\times(1+\varepsilon_a)}{1-\mu\varepsilon_a}\right). \quad (3)$$

The term axial strain factor (ASF) is introduced here to better describe the cable's axial strain behavior. The ASF is defined as the ratio of tape axial strain and CORC® cable axial strain. The ASF does not depend on applied axial strain. The main two factors that influence the ASF are the winding angle and the Poisson's ratio of the core. The influence of these parameters can be visualized by analytical equations, as shown in figure 4. CORC® cables with lower ASF possess higher tolerance towards the axial load.

An optimized CORC® cable should have an ASF close to zero; this can be achieved by using winding angles near 30° and by selecting a core material with a higher Poisson's ratio. Smaller winding angles can be achieved by using HTS tapes with smaller widths, or by reducing the gap size between tapes. For cables with negative ASF (shown in black in figure 4), the tape will experience a compressive strain or detach from the

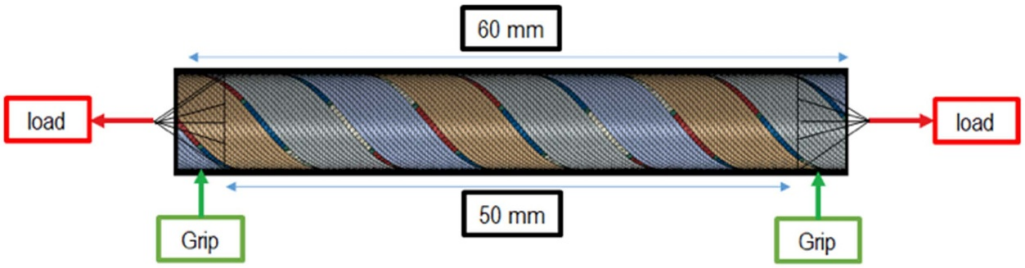

Figure 2. The boundary conditions for axial load applied to the CORC® cable.

Table 1. Material properties of Hastelloy C-276, copper, and REBCO [15].

	Young's modulus (GPa)	Yield stress (MPa)	Poisson ratio	Thermal expansion coefficient (K^{-1})
Hastelloy (RT)	223	891	0.307 [17]	1.34×10^{-5} [9]
Hastelloy (77 K)	228	1141	0.307 [17]	1.34×10^{-5} [9]
Copper (RT)	80	120	0.34 [18]	1.77×10^{-5} [9]
Copper (77 K)	98	146	0.34 [18]	1.77×10^{-5} [9]
REBCO (77 K and RT)	157 [19]	—	0.30 [19]	1.10×10^{-5} [9]

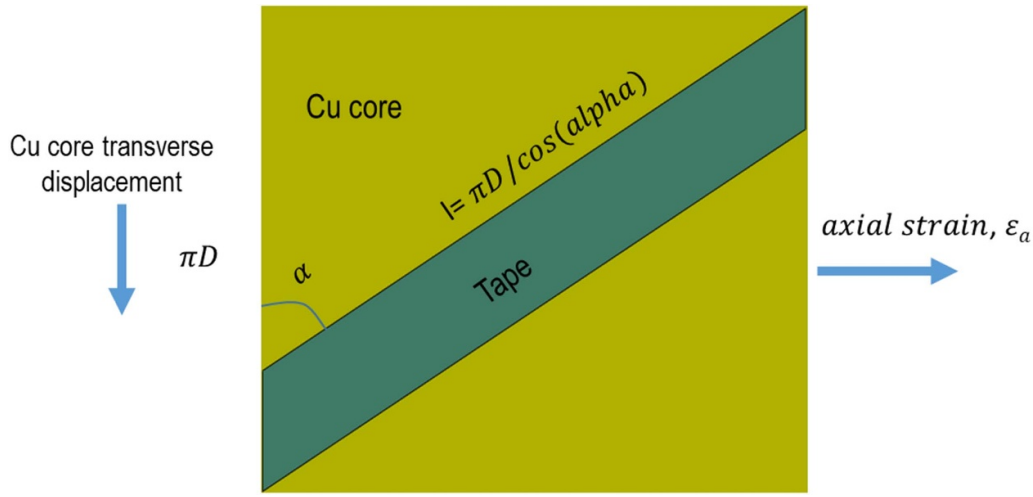

Figure 3. Schematic sketch of a CORC® cable in a rectangular plane for theoretical analysis of axial applied strain.

core if the periphery is not constrained. The cables with negative ASF can only get damaged by the high strain concentration near the cable ends where the tapes are constrained within the cable terminations. The damage process in small winding angle tapes is not by tensile load but by hard (out-of-plane) bending [21] of HTS tapes. The simple analytical model discussed above assumes a homogenous axial strain distribution within the tape and does not consider the strain concentration towards the cable ends. The axial tape strain can be used to calculate the critical current from equation (1). The effect of self-field is not considered for both Finite Element Method (FEM) and analytical model calculations. The FEM simulation data is only used to calculate the degradation of critical current (I_c/I_{c0}), not the absolute value. Since there is only one cable and the cable is straight throughout the process of axial load application, the cable is subjected to the same magnitude of self-field until the start of degradation. So, the effect of self-field in the critical current degradation is marginal; however, the absolute value of critical current depends upon the self-field.

3. Experimental validation

FE analysis was performed for four CORC® wires, manufactured and tested by Advanced Conductor Technologies LLC, with their details given in table 2. The coefficient of friction between all contact pairs in the FE simulation is taken as 0.2 [13].

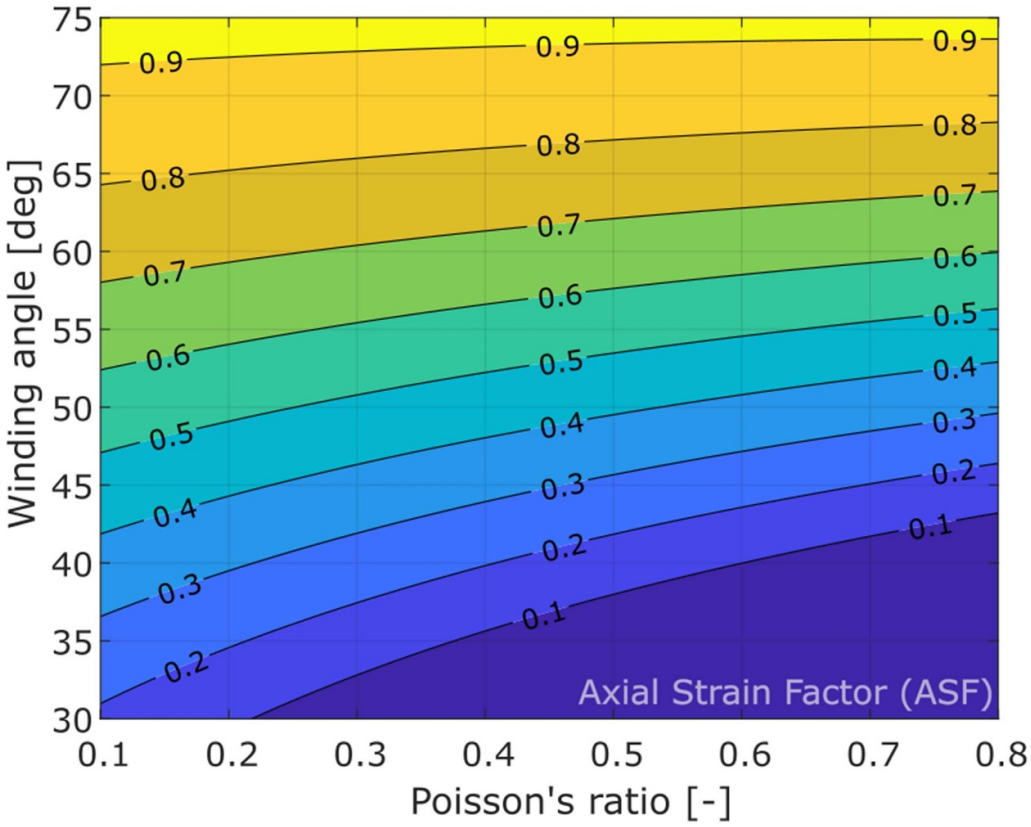

Figure 4. The variation in ASF as a function of Poisson's ratio and winding angle.

Table 2. Design parameters of CORC® wires [16].

	Number of tapes (-)	Tape width (mm)	Tape layers (-)	Core diameter (mm)	CORC® thickness (mm)	Tape winding angle (°)	Initial I_c (76 K) (A)
LA-CORC®	12	2	6	2.55	3.13	30–36	828
HA-CORC®	12	2	6	2.55	3.13	40–45	828
CORC®-S30	30	2	12	2.55	3.67	30–47	1710
CORC®-O28	28	2	14	2.55	3.81	25–35	1617

Two CORC® wires were selected for experimental validation of the models; LA-CORC® and HA-CORC®. Both LA-CORC® and HA-CORC® have the same design except for the winding angles; here LA and HA stands for low angle and high angle respectively. The data comparison between experimental, FEM, and analytical modeling results are shown in figure 5. The difference in the performance of these two wires indicates the influence of the winding angle on the CORC® wire axial loading behavior.

The FEM data show good agreement with the experimental data, and the analytical model shows a slight overestimation of the irreversible strain limit of the CORC® wire. Therefore, the FE model can predict the tensile strain behavior of CORC® wires with reasonable accuracy. However, the analytical model only provides a rough estimation of the performance due to its simplicity. The winding angle varies from 30° to 36° for the LA-CORC® wire and from 40° to 45° for the HA-CORC® wire. A reduction of 10° in winding angle increased the critical tensile strain limit from 1.5% for the LA-CORC® wire to 3.5% for the HA-CORC® wire as shown in figure 5.

CORC® wires are wound such that the innermost layer has the maximum winding angle, and the angle decreases towards the outermost layer. The contours of the axial strain and the normalized critical current for different layers of the HA-CORC® wire are shown in figures 6 and 7, respectively. The central copper core is hidden in figure 6 for better visibility of the HTS tape layers. The critical current contour is calculated using equation (1). An applied axial cable strain of 3.7%, larger than the cable's irreversible strain limit, is shown to visualize the irreversible damage in subsequent layers. The black stripes in the first two layers show the irreversible damage, i.e. cracks across the complete width of the HTS layer. Even at 3.7%, the outer layers of the CORC® wire are only slightly damaged due to the low winding angles.

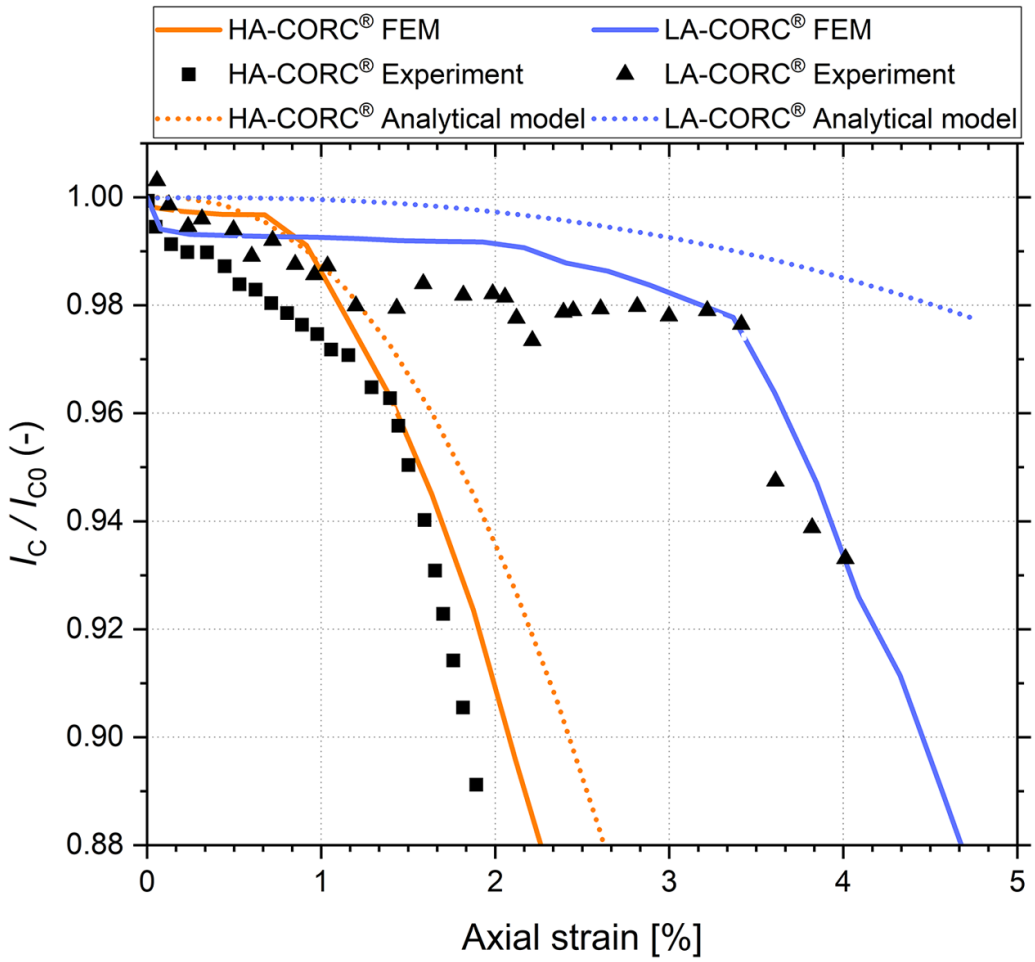

Figure 5. Comparison of experimental, FEM, and analytical modeling results for normalized critical current vs. axial tensile strain applied to CORC wires LA-CORC® and HA-CORC® from [16].

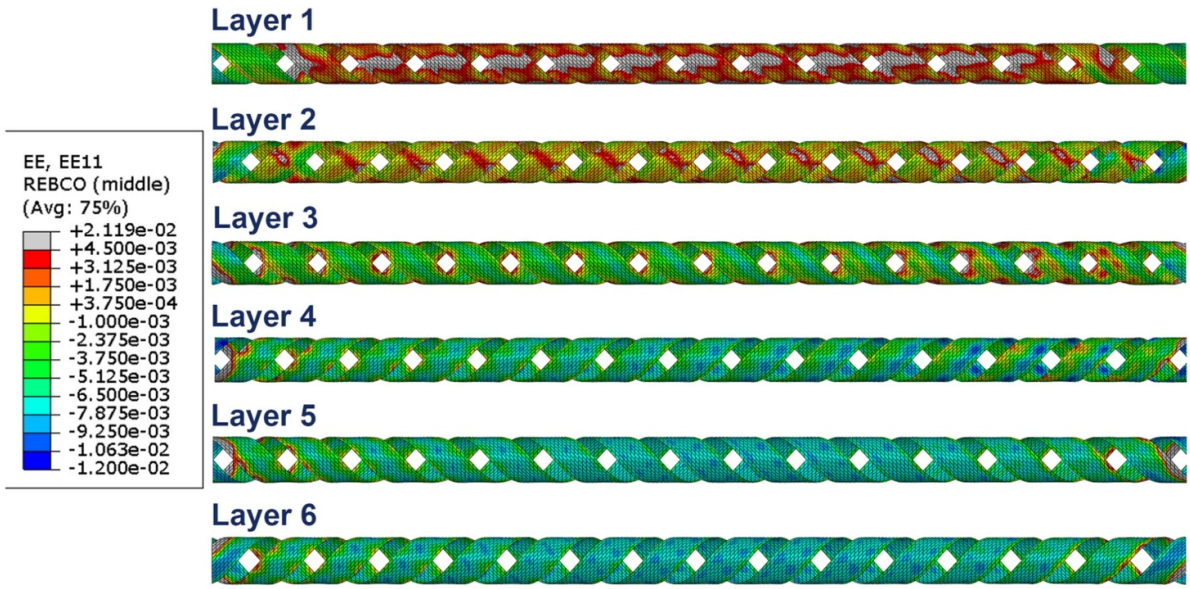

Figure 6. Axial strain contour for different layers of CORC® wire HA-CORC® at an applied axial strain of 3.7%. Gray areas correspond to locations where the intrinsic strain exceeded 0.45%.

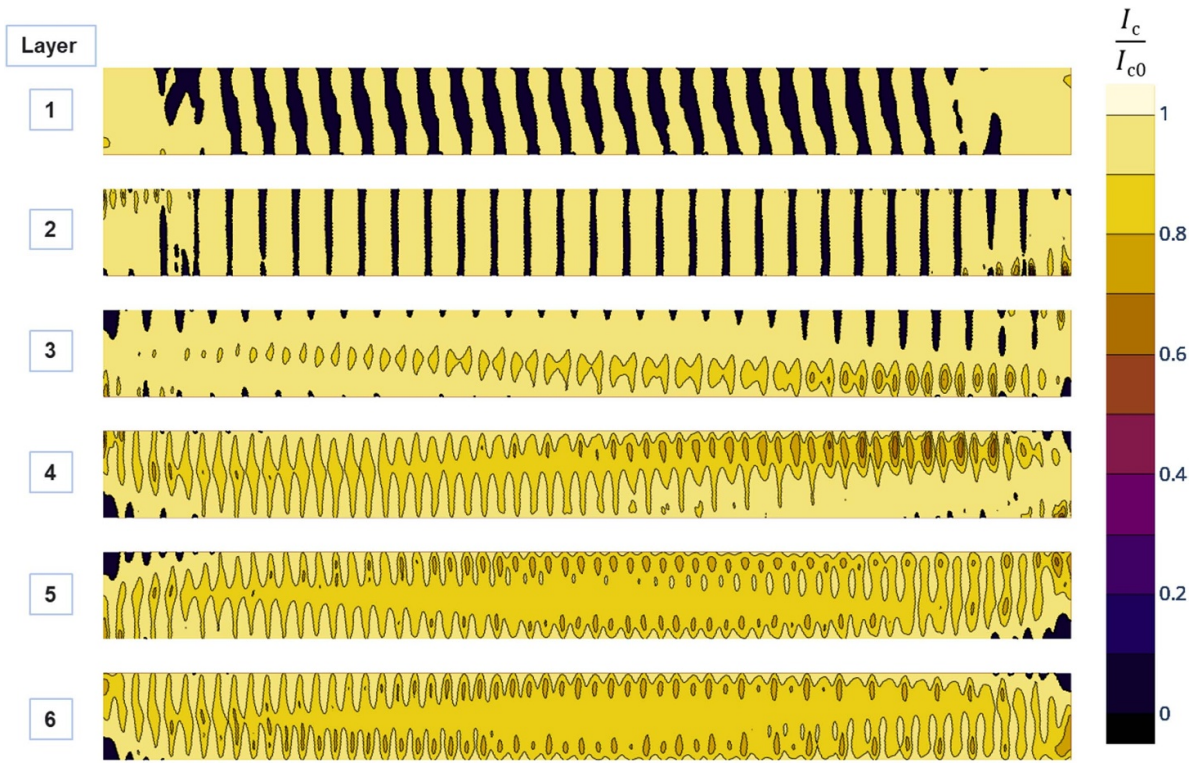

Figure 7. Normalized critical current (I_c/I_{c0}) contour for different layers of CORC® wire HA-CORC® at an applied axial tensile strain of 3.7%.

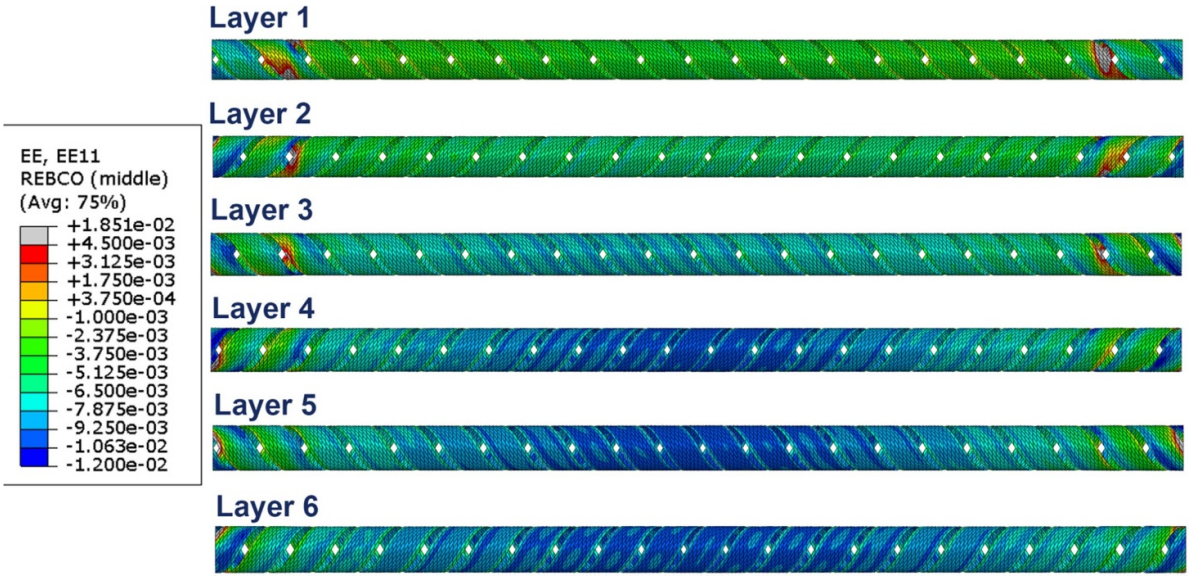

Figure 8. Axial strain contour for different layers of CORC® wire LA-CORC® at an applied axial tensile strain of 4.8%. Gray areas correspond to locations where the intrinsic strain exceeded 0.45%.

Figures 8 and 9 show the contours of the strain and critical current distribution in CORC® wire LA-CORC® at an applied tensile strain of 4.8%. Here only the inner two layers are showing cracks in the HTS layer. The cracks in the tapes start from the cable ends and then propagate to the cable center; this also confirms that the damage location for CORC® wires subjected to tensile strain is near the cable ends, as reported in [7].

4. Parametric analysis

Several FE simulations are carried out to better understand the effect of axial tensile strain on the performance of a single layer CORC® wire by changing various design parameters. The different parameters considered are winding angle, Poisson's ratio, core diameter, and tape width. In addition, the

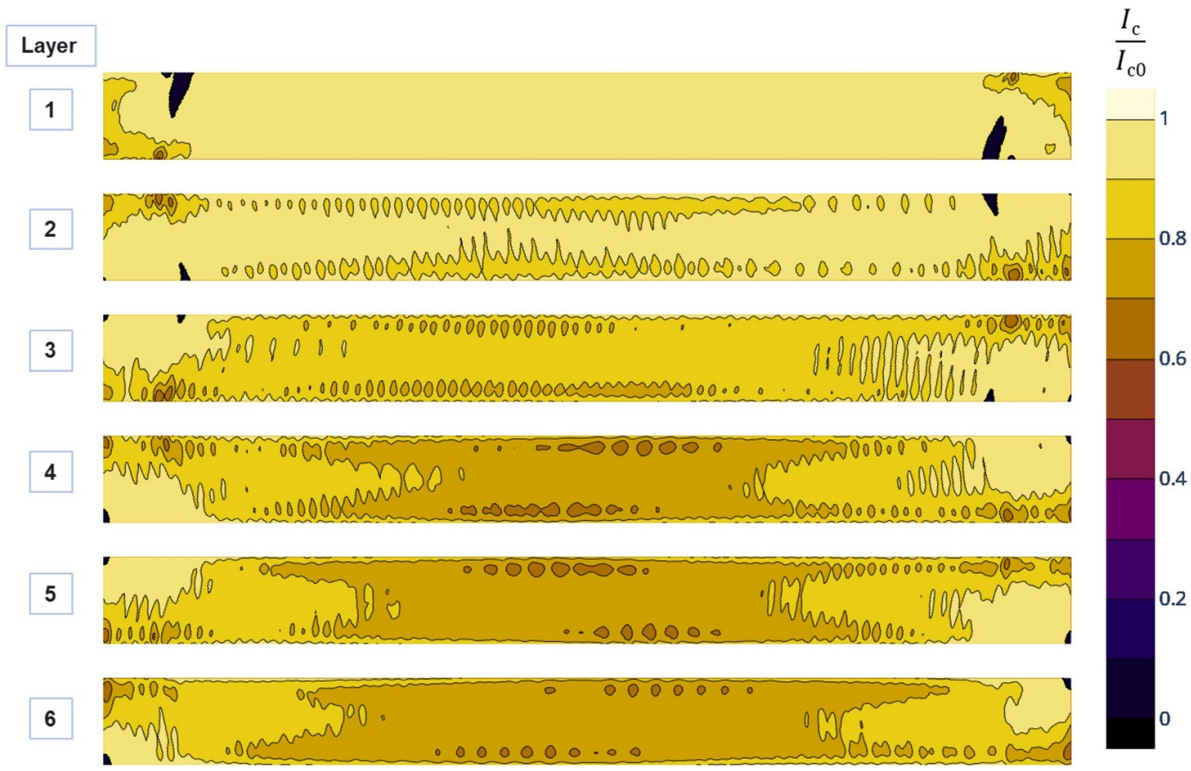

Figure 9. Normalized critical current (I_c/I_{c0}) contour for different layers of CORC® wire LA-CORC® at an applied axial tensile strain of 4.8%.

following parameters are kept constant for all simulations; the copper layer thickness plated onto the REBCO tapes as 5 μm, the Hastelloy substrate thickness of 30 μm, the friction coefficient of 0.2, the tensile tape load during winding of 10 N, the cable length of 60 mm, and both the number of tapes and layers as one.

4.1. Winding angle

Two sets of simulations are carried out: one without considering the production process and winding strain, and the other considering all mechanical loading steps. The first is to verify the analytical model results, and the second is to analyze the CORC® wire performance. In both cases, the winding angle is varied from 30° to 70°. A 3 mm wide tape and 3 mm diameter copper core is used in the FE simulations. Figure 10 shows the axial strain experienced by the REBCO tape at different winding angles for an applied CORC® wire strain of 1%. Here the FEM tape strain was obtained as the average tensile strain from the center of the tape. The FEM and analytical models show similar results.

The variation in normalized critical current as a function of applied CORC® wire strain for different winding angles is shown in figure 11. Increasing the winding angle reduces the tensile strain tolerance drastically, i.e. the critical current becomes more sensitive to applied strain at high winding angles. Therefore, the FE results confirm that the tapes' winding angle should be maintained close to ∼30° to have a higher tensile strain limit.

4.2. Poisson's ratio of the CORC® wire core

The Poisson's ratio of the CORC® wire core material controls the radial contraction of the core, as well as that for the tapes wound around the core, under axial tensile strain. Figure 12 shows how the Poisson's ratio influences the tensile load behavior of CORC® wires. The results shown here are for a winding angle of 35° at which the 3 mm wide tape was wound onto the 3 mm diameter core. The gap between the curves decreases significantly with increasing tape winding angle, i.e. the sensitivity of Poisson's ratio on the axial strain response decreases with an increase in winding angle (not shown in the figure). Even though the value of Poisson's ratio varied from 0.05 to 0.45 in this study, a more practical range for metals and alloys is between 0.25 and 0.35. For example, the Poisson's ratio of annealed copper is 0.343, that of beryllium copper is 0.30, and that of stainless steel is about 0.28.

The difference in radial contraction of the CORC® wire's core and the radial contraction of an unconfined (no core present) HTS tape wound into a helical form induces tensile strain in the REBCO layer. Therefore, an increase in Poisson's ratio of the core will increase its radial contraction, and therefore will impede the radial contraction of the HTS tapes to a lesser extent.

4.3. Core diameter

Another parameter that can influence the cable tensile load behavior is the core diameter, because it determines the initial strain state of the REBCO layer before axial load is applied.

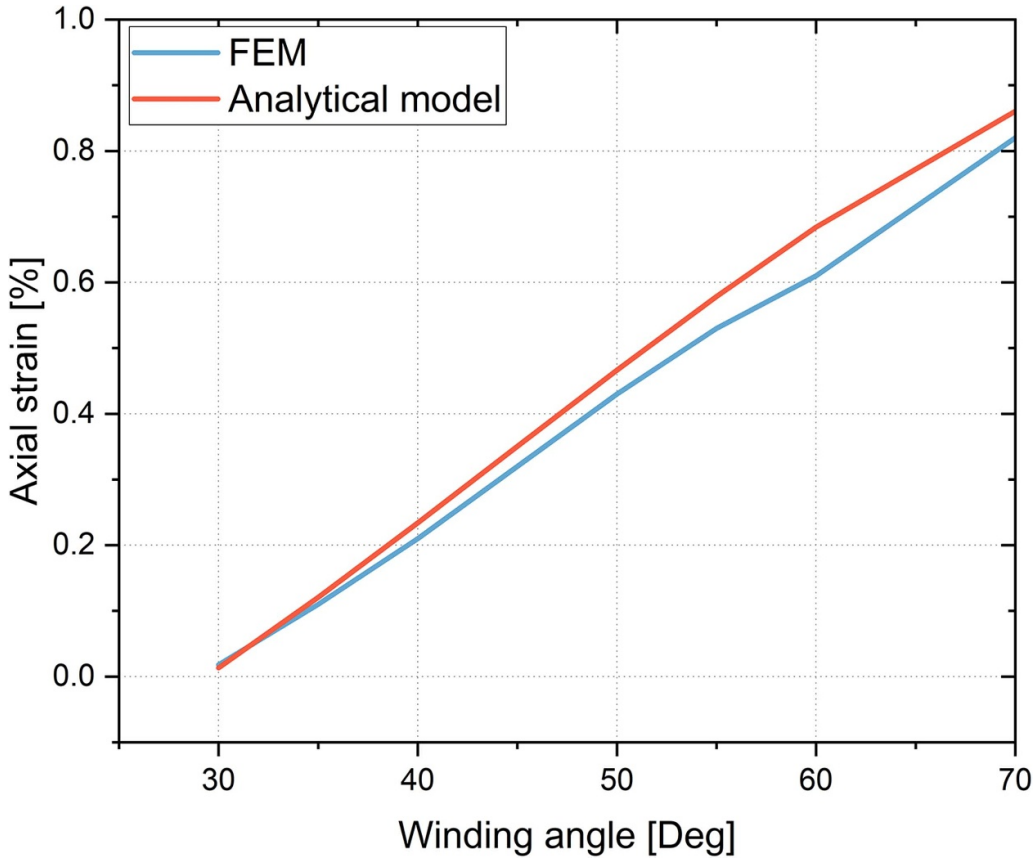

Figure 10. Average tape axial strain for different tape winding angles at an applied CORC® wire strain of 1%.

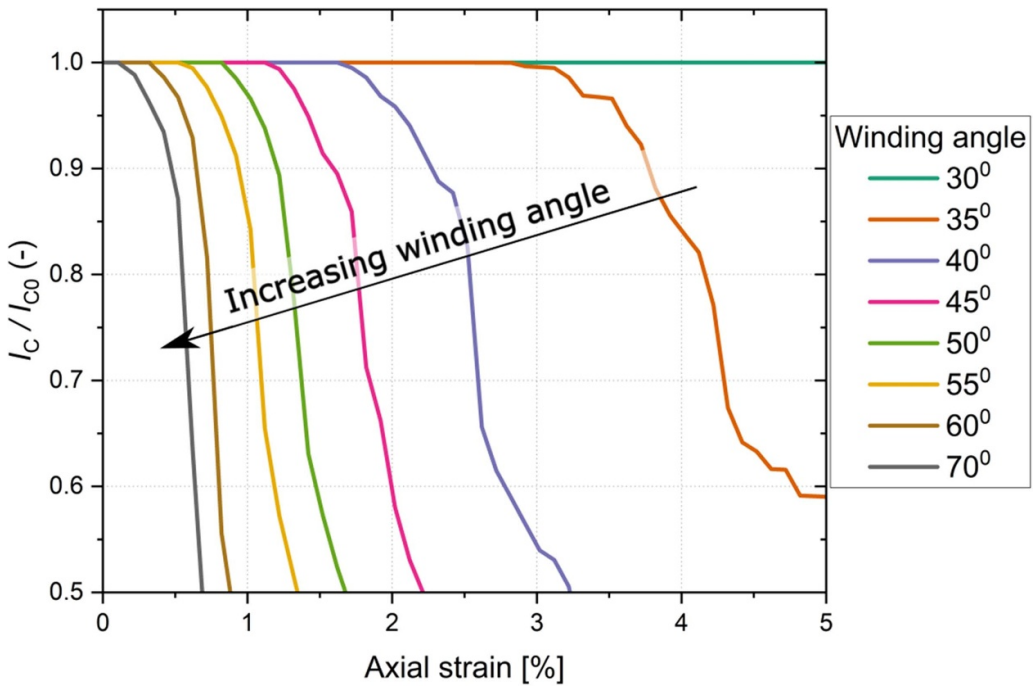

Figure 11. Effect of axial tensile strain on the normalized critical current of single layer CORC® wires at different winding angles.

If the core diameter is small, the compressive tensile strain of the REBCO layer will be higher, and the cable will require a higher applied tensile strain to reach the intrinsic tensile strain limit of 0.45%. Hence a cable with a smaller core diameter will have a higher tolerance to applied tensile strain. The FE model results for a 2 mm wide tape wound onto a core with different diameters is shown in figure 13, showing that the gaps between the curves narrow as the diameter of the core increases.

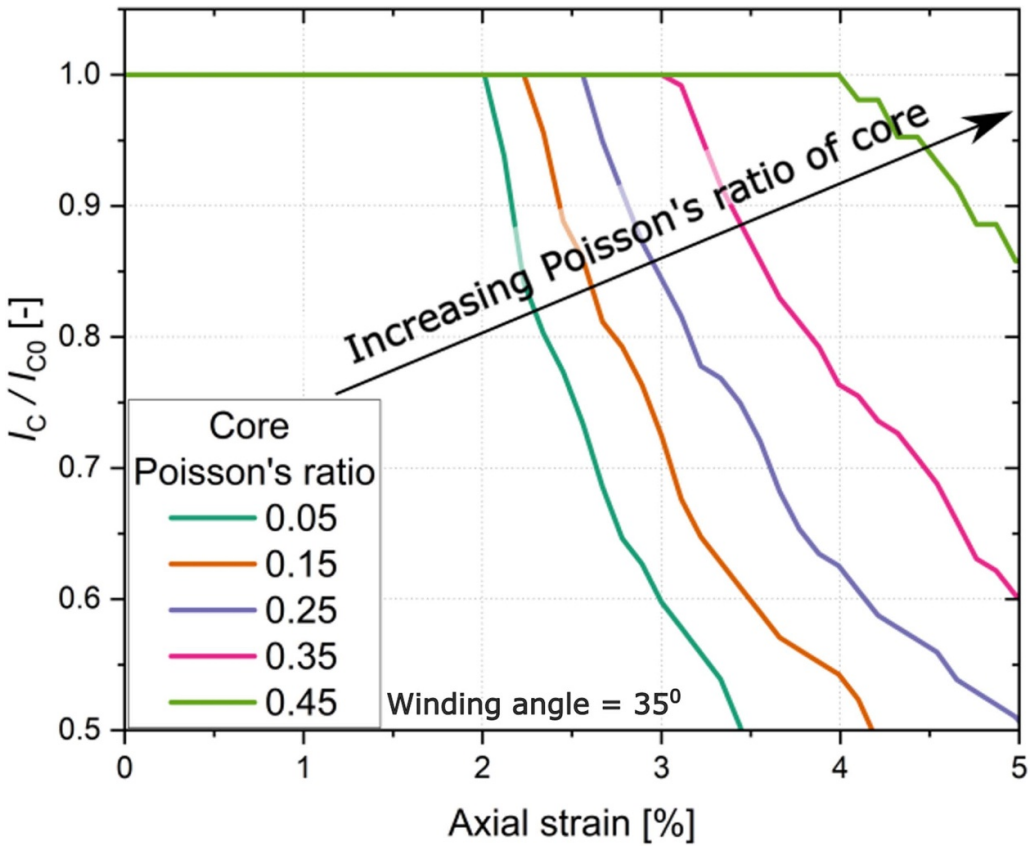

Figure 12. Effect of Poisson's ratio on the axial load performance of a single layer CORC® wire with a winding angle of 35°.

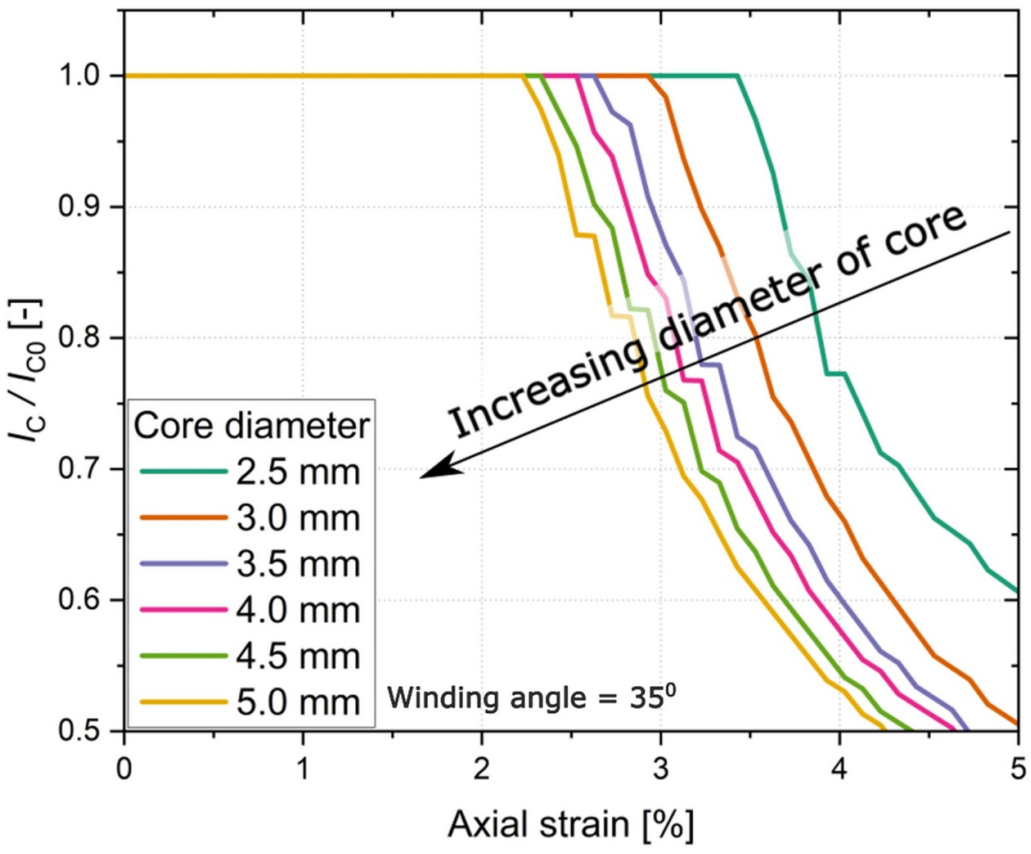

Figure 13. Effect of CORC wire® core diameter on the axial load performance of a single layer CORC® wire with a tape winding angle of 35°.

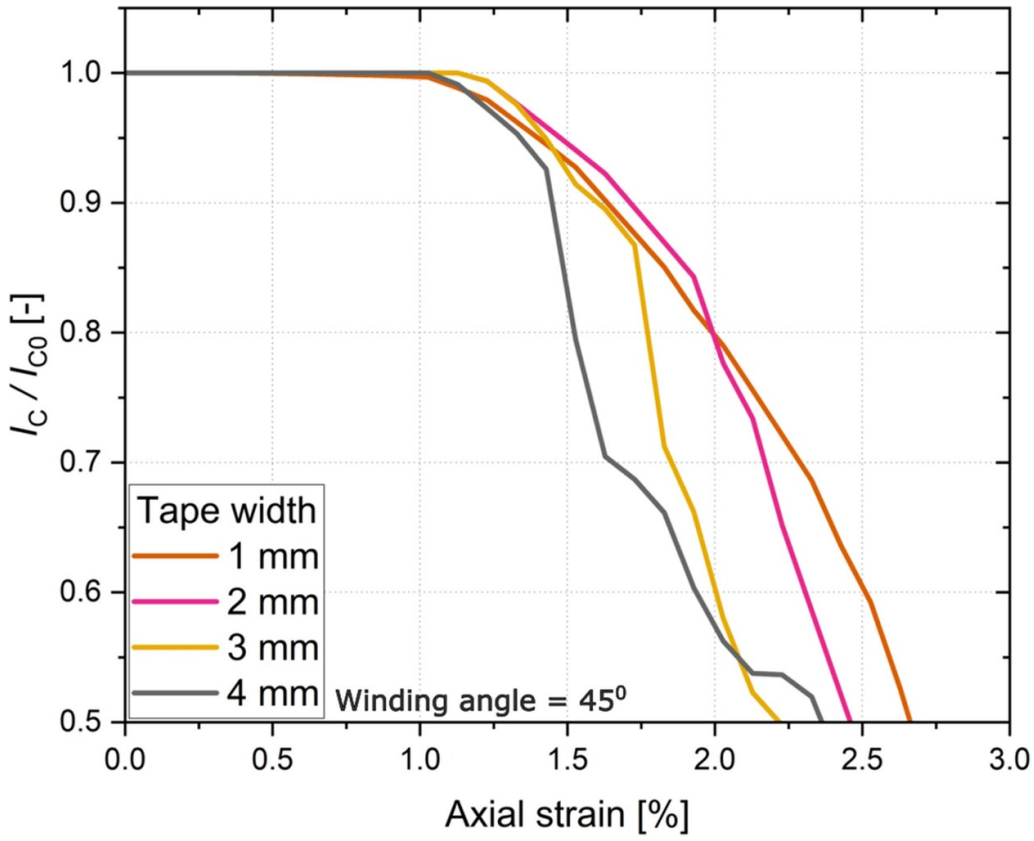

Figure 14. Effect of tape width on the axial load performance of a single layer CORC® wire with a winding angle of 45°.

4.4. Tape width

Another parameter that can influence the behavior of CORC® wires under tensile strain is the tape width. However, the influence of tape width seems to be marginal when all other parameters are kept the same, as shown in figure 14. A copper core with 3 mm diameter is used in all simulations. However, tapes with smaller widths can be wound at lower winding angles, increasing the tensile strain limit compared to wider tapes that need to be wound at a higher angle onto the same core. Hence, narrower tapes or larger core diameters allow smaller tape winding angles that results in a higher irreversible strain limit.

All the above parametric studies are performed for single-layer CORC® cables and wires. The presence of an additional layer can influence the tensile load behavior. The effect of an additional HTS layer is not the same as increasing the diameter. Top layers will exert transverse pressure onto the inner layers. The amount of contact pressure depends on the number of layers and the winding angle of individual layers.

5. Effect of layer interaction

Tapes in multilayered CORC® wires experience transverse load in addition to tensile, bending, and torsional loads. CORC® wire CORC®-S30 from [7] (table 2) was selected for FE analysis to investigate the layer-to-layer interaction under the application of axial tensile strain. This CORC® wire is suitable for studying the influence of layer interaction as both the winding angle and the number of tapes vary among the layers. The CORC® wire contains 30 tapes wound into 12 layers. The number of tapes in the first six layers is two, and in the outer six layers is three. The winding angle decreases from 36° to 30° in the first six layers and then from 47° to 40° in the outer six layers. Figure 15 shows the comparison between FEM, experiment, and the analytical model of the strain dependence of the normalized critical current of CORC® wire CORC®-S30. The FE analytical models show a good agreement with experimental data.

Figure 16 shows the critical current degradation of different layers of CORC® wire CORC®-S30. Here the experimental data points correspond to different tapes extracted from the CORC® wire after the experiment [7]; the I_c of each extracted tape is measured separately. Hence the experimental data points only show the irreversible damage as the tensile strain is mostly relieved while disassembling the CORC® wire. The FEM data shown in figure 16 correspond to an applied strain of 4.5%. It shows not only the critical current reduction from the irreversible damage but also the applied tensile strain. The experimental and FEM data show a similar trend in the reduction of the critical current. Layer 7 has the most damage, though it is predictable since it has the highest winding angle (46°); the interesting thing is that the 6th layer shows a large degradation in critical current even though the winding angle is the lowest (30°); this is the result of the complex layer-to-layer interaction within the multilayer CORC® wire.

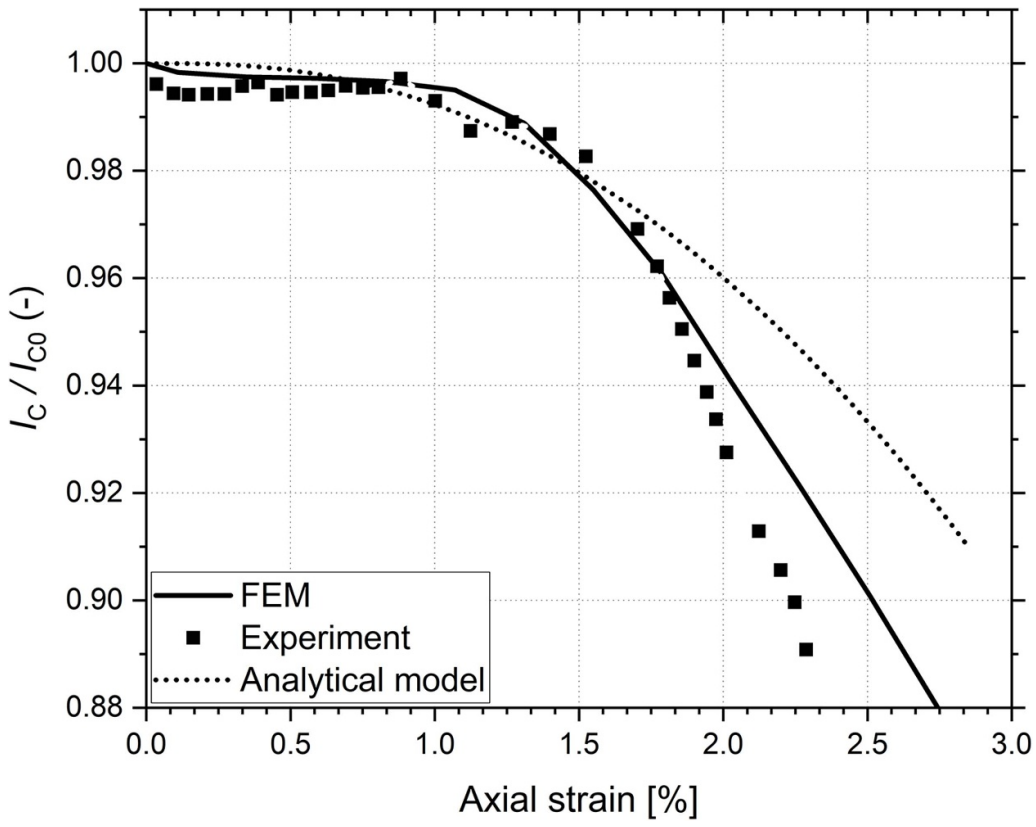

Figure 15. Comparison of the dependence of the normalized critical current on applied tensile strain measured in CORC® wire CORC®-S30 with FEM and analytical models.

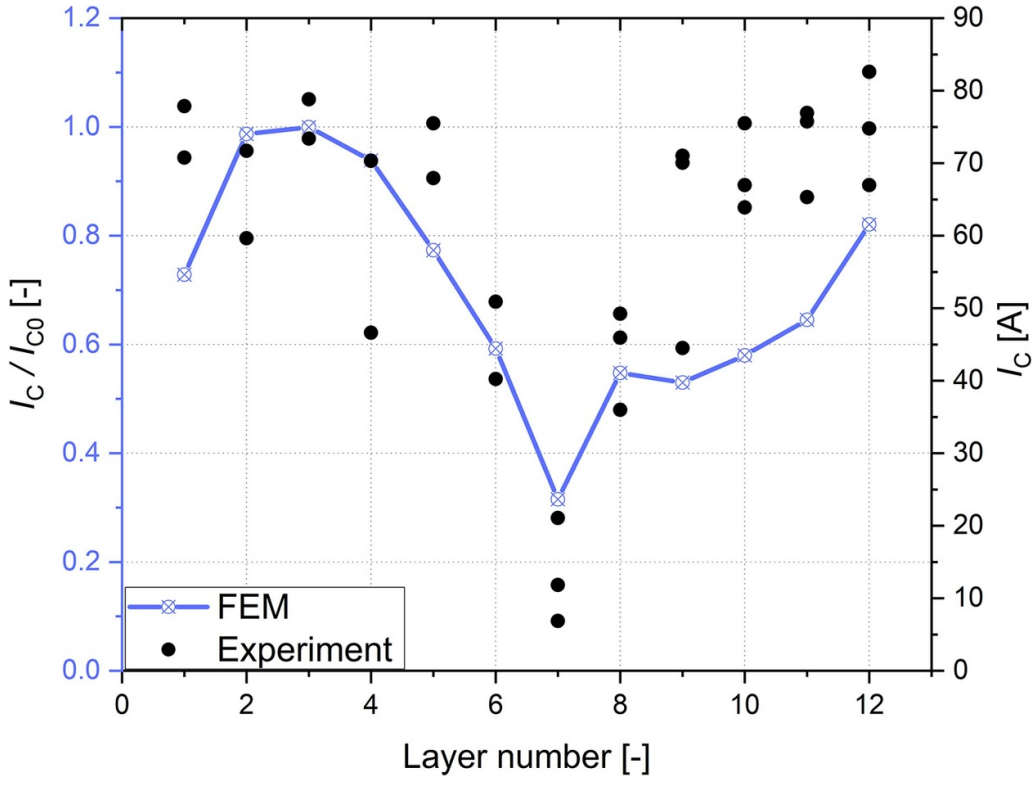

Figure 16. The critical current of tapes extracted from different layers of CORC® wire CORC®-S30 [7] and the calculated tape I_c using FEM.

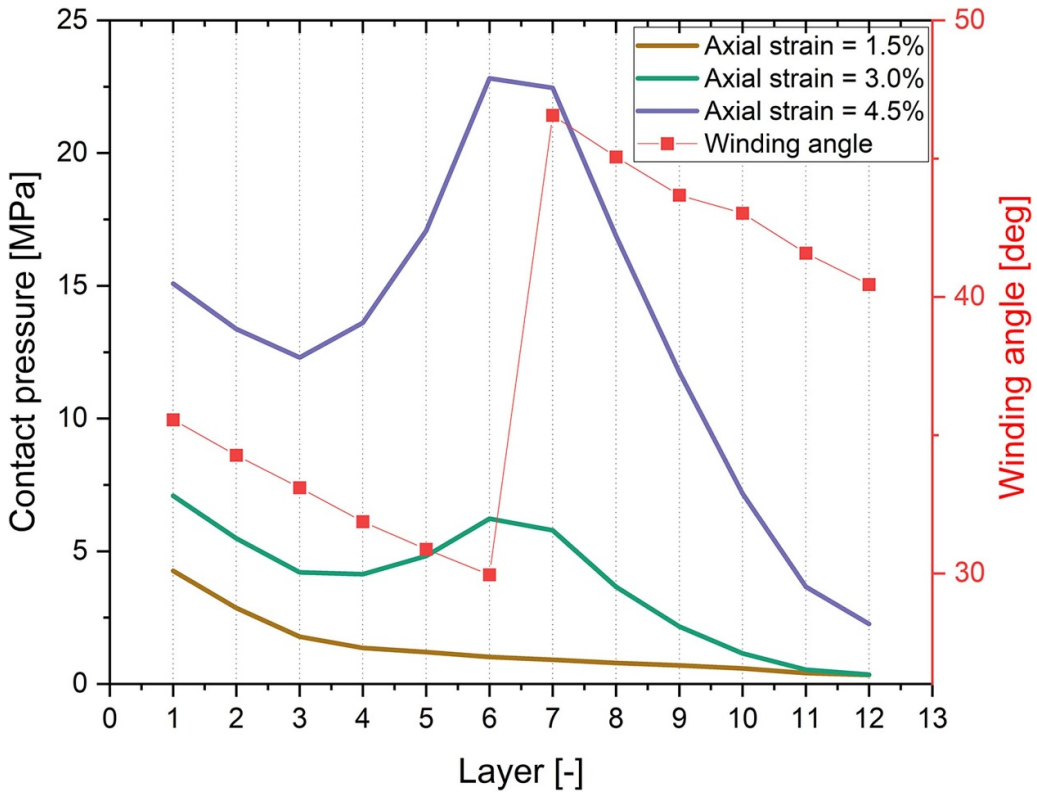

Figure 17. Contact pressure (FEM) on different layers of CORC® wire CORC®-S30 at different levels of applied CORC® wire axial tensile strain.

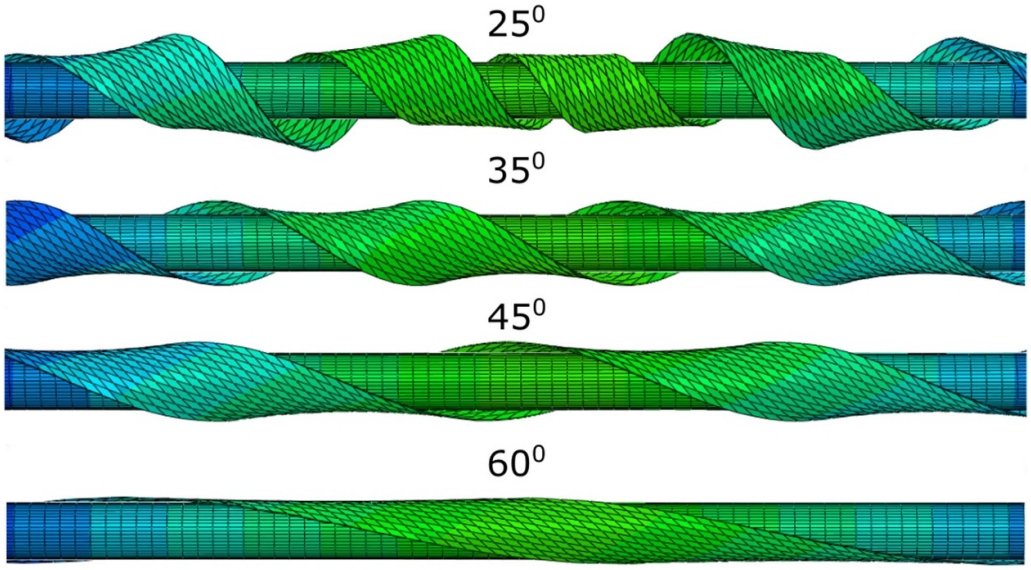

Figure 18. HTS tape deformation at different winding angles, deformation scale factor = 11, applied cable tensile strain = 10%.

The significant change in winding angle from 29° to 47° and the change in the number of tapes in the 7th layer, contributed to the reduction of the tape's critical current. The helical diameter of tapes with large winding angles contracts at a higher rate than the tapes with smaller winding angles. This difference in contraction causes the low winding angle tapes in the middle layer to experience significant transverse stresses from the neighboring layers. Figure 17 shows the contact pressure at different layers in the cable. This increased transverse pressure and the discontinuity in the cable layers are the main reasons for damage in layers 6–8. The 7th layer is damaged due to both transverse contact pressure and higher winding angles causing a higher tensile tape strain.

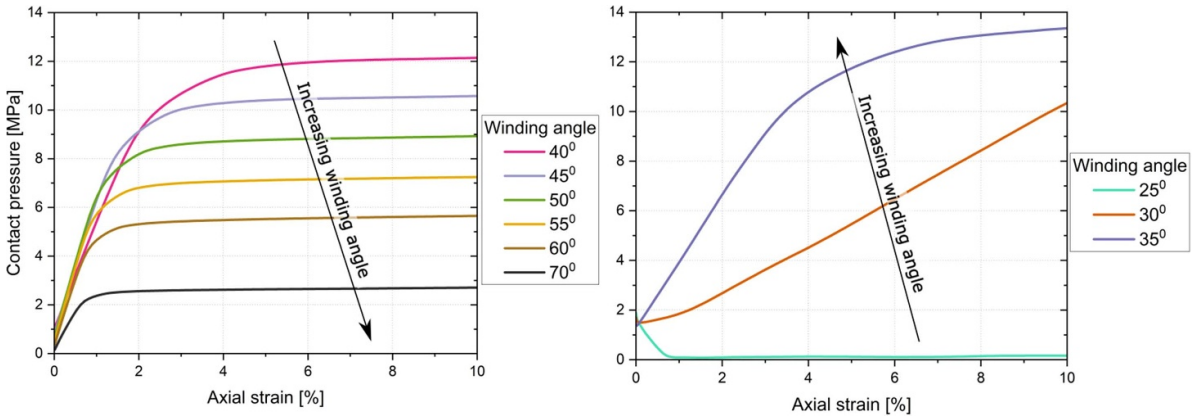

Figure 19. The contact pressure between the core and tape of a single layer CORC® wire wound at different winding angles; the data is shown in two figures to show the difference in the performance trend.

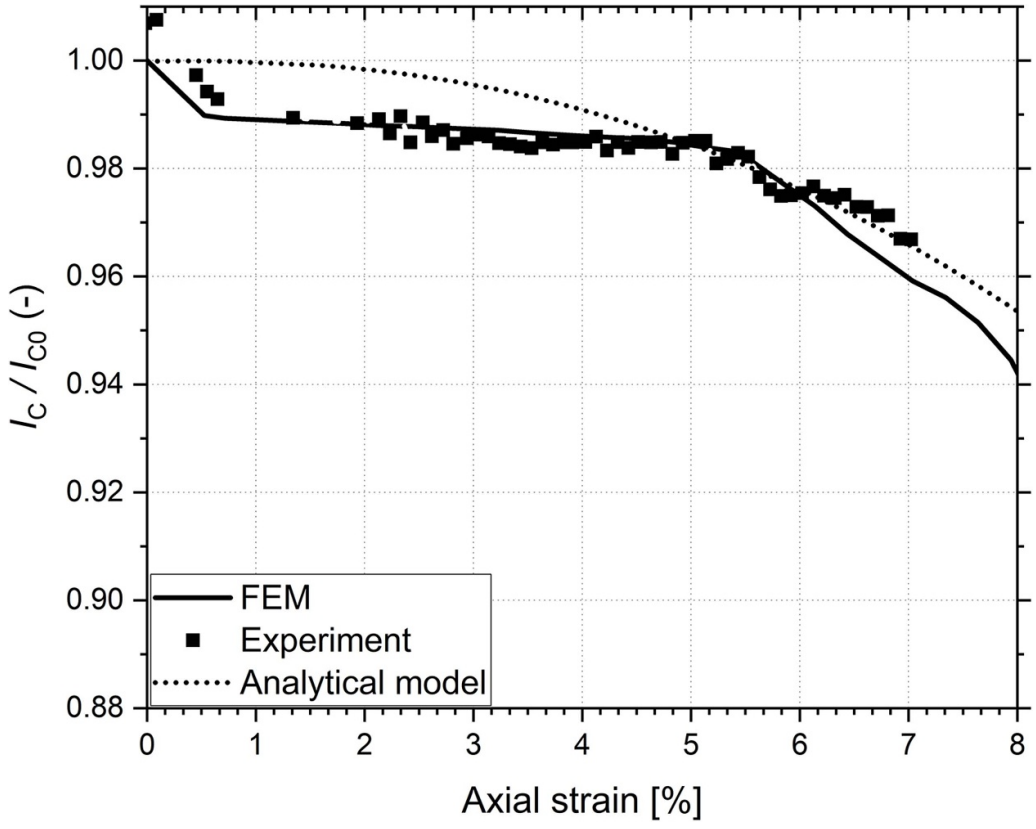

Figure 20. Normalized critical current as a function of applied axial tensile strain compared to FEM and analytical models for optimized CORC® wire CORC®-O28.

A series of FEM analyses are carried out to better understand the effect of tape winding angle on contact pressure. Figure 18 shows the tape deformation at different winding angles. For cables with winding angles corresponding to a negative ASF, the core contracts at a higher rate than the tape. As a result, the tape deforms at both sides of the CORC® wire and gets damaged by out-of-plane bending at large magnitudes of applied cable tensile strain. However, the presence of an additional layer can exert transverse pressure onto the tape and then cause early degradation. On the other hand, for cables with winding angles corresponding to a positive ASF, the tape contracts faster than the core; hence the tape experiences tensile strain. In addition, the deformation of the tape is concave across its width, and the concavity decreases with an increase in winding angle.

The rate of contraction increases the contact pressure between tapes. The contact pressure between tapes and the core for cables with different winding angles is shown in figure 19. The contact pressure increases and then saturates as the tape starts to deform plastically. The saturation contact pressure is lower for CORC® wires with higher winding angles as it undergoes plastic deformation first. However, for

CORC® wires with winding angles below 40°, the saturation contact pressure is not reached in the range of applied cable strain. For CORC® wires with a winding angle below 30°, the contact pressure decreases with applied axial strain as the tape detaches from the core but at the same time exerts additional stress onto the layers above. So, the contact pressure between layers of a multilayered cable at any applied axial strain shows a complicated behavior.

6. Cable design optimization

The irreversible strain limit under axial tensile strain of the multilayered CORC® wires can be increased by limiting the magnitude of the tape winding angle to 30° (for CORC® wires with annealed copper core) and by avoiding layer-to-layer discontinuities. The presence of additional layers increases the total contact pressure onto the first layer. A uniform decrease in winding angle towards the top layers can reduce the total contact pressure onto the first cable layer. Naturally, additional layers can be wound with lower winding angles than the layer below if the number of tapes per layer is kept constant. CORC® wire CORC®-O28 (table 2) [16] has optimized cable parameters with winding angles that vary from 25° to 35° towards the core. A comparison between experimental data from [16] and FEM and analytical models is shown in figure 20. The FEM and analytical models both show a good agreement with the experimental data. CORC® wire CORC®-O28 shows a tensile strain limit of about 7%, which is the highest for any superconducting cable so far.

7. Conclusion

A detailed CORC® wire FE model is developed to calculate the tape strain state as a function of axial tensile strain. The CORC® axial load FE model can predict the multilayer CORC® wire performance with reasonable accuracy. The analytical model for CORC® axial load indicates that the winding angle and Poisson's ratio are critical parameters that impact the tolerance to axial tensile strain of CORC® wires. The tolerance can be increased by reducing the tape winding angle, using a core with higher Poisson's ratio, and by decreasing the core's diameter. The effect of the tape width on the tensile strain limit is only marginal. The FE model results also show that layer-to-layer interaction plays a major role in the axial load performance of CORC® wires, which is confirmed by experimental data. The contact pressure between layers of multilayered CORC® wires can increase significantly between layers in which the tape winding angle suddenly changes, which is the case when the number of tapes wound into a single layer changes. This results in additional tape degradation within these layers. The cable design can be significantly optimized by choosing the right range of winding angles and by keeping the number of tapes wound in each layer the same. With optimized cabling parameters, the irreversible strain limit under axial tension of CORC® cables and wires can be as high as 7%, which is 10–12 times higher than the irreversible strain limit of single REBCO tapes.

Data availability statement

All data that support the findings of this study are included within the article (and any supplementary files).

Acknowledgments

Part of the work is supported by the University of Twente, Enschede, the Netherlands and by the United States Department of Energy, Offices of High Energy Physics and Fusion Energy Sciences under Grant Numbers DE-SC0014009, DE-SC0018125 and DE-SC0020710. Part of this work has been carried out within the framework of the EUROfusion Consortium and has received funding from the Euratom research and training program 2014–2018 and 2019–2020. The views and opinions expressed herein do not necessarily reflect those of any of the above-acknowledged parties.

ORCID iDs

V A Anvar https://orcid.org/0000-0003-1264-6442
K Wang https://orcid.org/0000-0001-5858-5396
D C van der Laan https://orcid.org/0000-0001-5889-3751
M S A Hossain https://orcid.org/0000-0002-5588-0354
A Nijhuis https://orcid.org/0000-0002-1600-9451

References

[1] Creely A J *et al* 2020 Overview of the SPARC tokamak *J. Plasma Phys.* **86** 865860502
[2] Mitchell N *et al* 2021 Superconductors for fusion: a roadmap *Supercond. Sci. Technol.* **34** 103001
[3] Zhai Y, van der Laan D, Connolly P and Kessel C 2021 Conceptual design of HTS magnets for fusion nuclear science facility *Fusion Eng. Des.* **168** 112611
[4] Takayasu M, Chiesa L, Allen N C and Minervini J V 2016 Present status and recent developments of the twisted stacked-tape cable conductor *IEEE Trans. Appl. Supercond.* **26** 25–34
[5] Goldacker W, Grilli F, Pardo E, Kario A, Schlachter S I and Vojenčiak M 2014 Roebel cables from REBCO coated conductors: a one-century-old concept for the superconductivity of the future *Supercond. Sci. Technol.* **27** 093001
[6] van der Laan D C, Weiss J D and McRae D M 2019 Status of CORC® cables and wires for use in high-field magnets and power systems a decade after their introduction *Supercond. Sci. Technol.* **32** 033001
[7] van der Laan D C, McRae D M and Weiss J D 2019 Effect of monotonic and cyclic axial tensile stress on the performance of superconducting CORC® wires *Supercond. Sci. Technol.* **32** 054004
[8] van der Laan D C, McRae D M and Weiss J D 2019 Effect of transverse compressive monotonic and cyclic loading on the performance of superconducting CORC® cables and wires *Supercond. Sci. Technol.* **32** 015002
[9] Osamura K, Sugano M, MacHiya S, Adachi H, Ochiai S and Sato M 2009 Internal residual strain and critical current maximum of a surrounded Cu stabilized YBCO coated conductor *Supercond. Sci. Technol.* **22** 65001

[10] van der Laan D C 2009 $YBa_2Cu_3O_{7-d}$ coated conductor cabling for low ac-loss and high-field magnet applications* *Supercond. Sci. Technol.* **22** 065013
[11] Weiss J D, Mulder T, ten Kate H J and van der Laan D C 2017 Introduction of CORC® wires: highly flexible, round high-temperature superconducting wires for magnet and power transmission applications *Supercond. Sci. Technol.* **30** 014002
[12] Weiss J D, van der Laan D C, Hazelton D, Knoll A, Carota G, Abraimov D, Francis A, Small M A, Bradford G and Jaroszynski J 2020 Introduction of the next generation of CORC® wires with engineering current density exceeding 650 A mm^{-2} at 12 T based on SuperPower's ReBCO tapes containing substrates of 25 μm thickness *Supercond. Sci. Technol.* **33** 044001
[13] Anvar V A *et al* 2018 Bending of CORC® cables and wires: finite element parametric study and experimental validation *Supercond. Sci. Technol.* **31** 115006
[14] Wang K and Gao Y 2020 The contact behavior of the CORC wires under stretching process *IEEE Trans. Appl. Supercond.* **30** 6601105
[15] Ilin K, Yagotintsev K A, Zhou C, Gao P, Kosse J, Otten S J, Wessel W A J, Haugan T J, van der Laan D C and Nijhuis A 2015 Experiments and FE modeling of stress-strain state in ReBCO tape under tensile, torsional and transverse load *Supercond. Sci. Technol.* **28** 55006
[16] van der Laan D C, Radcliff K, Anvar V A, Wang K, Nijhuis A and Weiss J D 2021 High-temperature superconducting CORC® wires with record-breaking axial tensile strain tolerance present a breakthrough for high-field magnets *Supercond. Sci. Technol.* **34** 10LT01
[17] Special Metals Corporation 2004 Publication number SMC019 (available at: www.specialmetals.com/documents/technical-bulletins/inconel/inconel-alloy-c-276.pdf (2004))
[18] Freund L B and Suresh S 2003 *Thin Film Materials: Stress, Defect Formation, and Surface Evolution* (Cambridge: Cambridge University Press)
[19] Cheon J H, Shankar P S and Singh J P 2005 Influence of processing methods on residual stress evolution in coated conductors *Supercond. Sci. Technol.* **18** 142–6
[20] van der Laan D C and Ekin J W 2007 Large intrinsic effect of axial strain on the critical current of high-temperature superconductors for electric power applications *Appl. Phys. Lett.* **90** 052506
[21] Fu Y, Wang Y, Hou Y, Kan C and Zhang H 2017 Out-of-plane bending characteristics of second generation high temperature superconducting tapes *Supercond. Sci. Technol.* **30** 075009